

Article

Three-Dimensional Iterative Enhancement for Coverage Hole Recovery in Underwater Wireless Sensor Networks

Lingli Zhang ¹, Chengming Luo ², Xiyun Ge ³, Yuxin Cao ⁴, Haobo Zhang ² and Gaifang Xin ^{5,*}

¹ College of Automation, Jiangsu University of Science and Technology, Zhenjiang 212100, China; zll_1030@163.com

² Ocean College, Jiangsu University of Science and Technology, Zhenjiang 212100, China; chengmingluo@126.com (C.L.); 211210301423@stu.just.edu.cn (H.Z.)

³ China Ship Scientific Research Center, Wuxi 214081, China; gexiyuncumt@163.com

⁴ Tsinghua Shenzhen International Graduate School, Tsinghua University, Shenzhen 518000, China; caoyx21@mails.tsinghua.edu.cn

⁵ Department of Intelligent Equipment, Changzhou College of Information Technology, Changzhou 213164, China

* Correspondence: xingaifang@ccit.js.cn

Abstract: The efficient coverage of underwater wireless sensor networks (UWSNs) has become increasingly important because of the scarcity of underwater node resources. Complex underwater environments, water flow forces, and undulating seabed reduce the coverage effect of underwater nodes, even leading to coverage holes in UWSNs. To solve the problems of uneven coverage distribution and coverage holes, a three-dimensional iterative enhancement algorithm is proposed for UWSN coverage hole recovery using intelligent search followed by virtual force. Benefiting from biological heuristic search algorithms, improved particle swarm optimization is applied for node pre-coverage. With the change in iteration times, the adaptive inertia weight, acceleration factor, and node position are constantly updated. To avoid excessive coverage holes caused by search falling into local optimum, underwater nodes are considered as particles in the potential field whose virtual forces are calculated to guide nodes towards higher coverage positions. In addition, based on the optimal node location obtained by the proposed algorithm, the monitoring area is divided based on the clustering idea. The underwater routing protocol DBR based on depth information is subsequently used to optimize node residual energy, and its average is calculated comprehensively and compared with the other three coverage algorithms using the DBR routing protocol. Based on the experimental data, after 100 iterations, the coverage rates for BES, 3D-IVFA, DABVF, and the proposed algorithm are 83.28%, 88.85%, 89.31%, and 91.36%, respectively. Moreover, the proposed algorithm is further verified from the aspects of different node numbers, coverage efficiency, node movement trajectory, coverage hole, and average residual energy of nodes, which provides conditions for resource development and scientific research in marine environments.

Keywords: UWSNs; node three-dimensional deployment; iterative enhancement; coverage hole recovery; node action force



Citation: Zhang, L.; Luo, C.; Ge, X.; Cao, Y.; Zhang, H.; Xin, G. Three-Dimensional Iterative Enhancement for Coverage Hole Recovery in Underwater Wireless Sensor Networks. *J. Mar. Sci. Eng.* **2023**, *11*, 2365. <https://doi.org/10.3390/jmse11122365>

Received: 15 November 2023

Revised: 8 December 2023

Accepted: 9 December 2023

Published: 14 December 2023



Copyright: © 2023 by the authors. Licensee MDPI, Basel, Switzerland. This article is an open access article distributed under the terms and conditions of the Creative Commons Attribution (CC BY) license (<https://creativecommons.org/licenses/by/4.0/>).

1. Introduction

With the continuous exploitation of marine resources, underwater wireless sensor networks (UWSNs) composed of underwater nodes have made great achievements in disaster warning, target tracking, and other fields [1]. In the target region of the UWSNs, nodes obtain the required data through the Internet of underwater devices [2]. These underwater nodes have data acquisition, transmission, and communication capabilities for the interaction of physical and logical information via hydroacoustic signals [3]. The ability of underwater acoustic communication is correlated with channel, transmission power, array, etc., and the quality of underwater acoustic communication is usually measured as

the product of underwater communication rate and distance. According to statistics from the US Naval Research Laboratory, the product of most underwater acoustic communication rates and distances is $40 \text{ kbps} \times \text{km}$, which means the maximum communication distance at a communication rate of 40 kbps is 1 km. In 2020, Zhejiang University reported a communication distance of 6.2 km and a communication speed of 42.8 kbps under a ship speed of 4–6 knots, with a product of $265.36 \text{ kbps} \times \text{km}$ long-distance communication. It is well known that hydroacoustic perception is superior to other sensing methods [4]. Hence, reasonable deployment of underwater nodes based on hydroacoustic communication is the basis of realizing efficient network monitoring [5]. Usually, random deployment results in a poor distribution density balance of nodes, resulting in coverage holes in UWSNs that cannot be effectively connected. When the network is not connected, the ground receiving station and the underwater node cannot communicate normally, and the data cannot be obtained, thus causing partial paralysis of the UWSNs [6]. Limited by the actual cost of underwater hardware, deploying as few sensors as possible to collect more information is an ideal option that has usually been pursued [7]. Underwater node location is crucial to the network coverage effect, and it needs to be updated constantly to complete the monitoring task. Achieving a maximum coverage rate for carrying out online monitoring is very important for improving the quality of services in UWSNs [8].

Some scholars have conducted a series of in-depth research on node coverage control. Considering the covering angle of nodes, a dynamic node deployment model with two-dimensional distribution was proposed to transmit the aggregated data, but it did not consider how the sensor node drift would be affected by water flow in dynamic open waters [9]. To address the coverage black hole caused by node drifts, a virtual force is introduced to drive the underwater sensor node to repair the covering black hole, and the boundary of the black hole is obtained using a geometric solution [10]. However, the motion of the sensor node perpendicular to the ground is ignored. Zhang et al. used the depth direction mobility of nodes for topology optimization and designed corresponding optimization criteria [11]. Wang et al. anchored the nodes randomly on the seabed; the nodes can move in the depth direction. On the premise of ensuring mutual communication, a weighted complete bipartite graph is generated to simulate the coverage of each node [12]. The scheme with the minimum number of nodes obtained using the cooperative path topology achieved target optimization, and a coverage strategy of limited and full communication redundancy was obtained [13]. Considering the coverage black hole problem in three-dimensional environments, Wei et al. used the semicircular plate rotation method to transform the two-dimensional coverage problem into a three-dimensional coverage problem [14]. The proposed strategy is feasible within the aquatic boundary. Given the three-dimensional environment, especially when there exists water flow and obstacles underwater, it is necessary to consider the optimal coverage scheme of underwater nodes in three-dimensional space under the condition of balanced network coverage performance.

Intelligence optimization algorithms have prompted researchers to propose innovative techniques capable of improving coverage performance [15]. After transforming node coverage and energy problems into octahedral task allocation problems, Zhao et al. proposed a vampire bat optimizer method, which enhanced coverage efficiency and reduced energy consumption [16]. As the water moves, the nodes change position, making UWSNs prone to dynamic topology drifts. To solve the coverage problem in an underwater dynamic environment and with depth information as the preferred selection condition, the optimal deployment was selected using a strategy of obtaining the optimal solution step by step; this was also effective for irregularly distributed underwater nodes [17]. To directly improve the global search capability for obtaining global optimal coverage, Zhang et al. utilized an enhanced fruit fly optimization algorithm to reasonably adjust node positions [18]. Fattah et al. combined the advantages of adaptive multi-parent crossover and fuzzy dominance to balance UWSN performance, including coverage rate [19]. However, it is difficult for the UWSNs to achieve a balance in coverage, node energy consumption, and execution time. Kapileswar et al. adopted a bald eagle search (BES) to optimize the entire UWSN

performance [20]. Node battery replacement is challenging and demanding in changing underwater environments. We need to pay attention to the loss of energy generated by nodes in the networks in the flow to maintain its stability. Overly complex optimization algorithms are prone to falling into local optima and cannot maximize coverage rates.

Many scholars regard underwater nodes as particles and adjust their locations by calculating the forces between particles, thereby reducing the coverage holes. Considering the limited underwater node resources, Jiang et al. conducted a three-dimensional redeployment of underwater mobile nodes based on virtual forces between nodes and utilized water flow forces to reduce energy consumption [21]. Unlike the conventional calculation of attraction and repulsion between nodes, some scholars proposed a three-dimensional improved virtual forces algorithm (3D-IVFA) by introducing central gravity and equilibrium force. The algorithm was proved to be effective in terms of coverage and uniformity [22]. One NP problem for achieving optimal network coverage performance with fewer nodes is the *K*-coverage problem. Wang et al. propose an improved virtual force algorithm (VFA) combined with the radius method of the same utility to solve a variety of *K*-cover optimization problems with varying coverage densities [23]. Due to the inability to predict underwater node locations, centralized node deployment makes it difficult to achieve effective coverage. A distributed algorithm based on virtual forces (DABVFs) was utilized to enhance the coverage rate of regions of interest, while the issue of coverage holes caused by underwater faulty nodes was also considered [24]. Of course, some scholars have also focused on the issue of a relatively small number of underwater nodes covering key areas of interest and proposed the focus virtual force field method [25]. Some scholars tried to combine particle swarm optimization algorithms with virtual force to enhance UWSN coverage performance. Hu et al. used the virtual forces between particles to guide particle optimization, accelerating particle convergence to the best overall solution and achieving the best coverage value [26]. All the above methods can improve the UWSN coverage, but these algorithms are prone to oscillations in the later stages and uneven coverage due to poor stability. As discussed, this study reviews the research on coverage of wireless sensor networks in 2D and 3D environments using intelligent optimization algorithms and compares coverage algorithms in the literature. The results are shown in Table 1.

Table 1. Comparisons of coverage optimization algorithms.

Surveyed Works	Proposed Method	Solved Problem	Advantages
So-In, C., 2019 [10]	CHHA	Coverage holes	Apply virtual force under Delaunay triangulation.
Yao, Y., 2022 [15]	VF-IMFO	Coverage holes	Analyze virtual force for node path optimization.
Zhao, X.Q., 2019 [16]	VBO	Energy consumption	Multi-energy optimization during redeployment.
Yi, J., 2023 [17]	IGS	Node coverage	Transform coverage problem into multiple local optimal.
Zhang, Y., 2017 [18]	UFOA	Node coverage	Optimal coverage under drosophila foraging behavior.
Jiang, P., 2018 [21]	VFRBEC	Node coverage	Correct node displacement underwater flow force.
Wang, W., 2019 [23]	k-ERVFA	<i>k</i> -coverage	An uneven coverage for <i>k</i> -coverage requirements.
Liu, C., 2019 [24]	DABVF	Node coverage	Node virtual force and fault judgment mechanism.
Hu, Y., 2022 [26]	VF-PSO	Node coverage	Optimize network coverage and distance threshold.

Given the non-universal seawater environment, nodes in the underwater environment are generally difficult to replace; their power supplies are also generally difficult to charge. The energy problem directly affects the service life of the entire sensor network. At present, many reliable and energy-saving underwater communication routing protocols are applied to solve energy loss by UWSNs. Peng et al. designed a routing protocol with the help of vector position information. By obtaining node coordinate information, packets are forwarded in the virtual channel established between the sending node and the receiving node. However, when the distribution of nodes is sparse, there may be a next receiving node in the pipeline that cannot meet the forwarding conditions, leading to an interruption of the communication path [27]. In response to this problem, Wang et al. put forward an improved HH-VBF scheme, which re-establishes a vector pointing to the destination node

on each hop forwarding node, calculates its distance to the vector hop by hop, and compares it with a specified threshold to determine whether to forward the packet. The strategy of changing the routing vector by hop number alleviates the problem of unbalanced energy consumption of network nodes to some extent [28]. However, since a routing pipeline is still used, it is still possible that the next hop node does not exist. Ref. [29] used depth information as a condition for routing and forwarding. However, since node depth is the only forwarding parameter, nodes with smaller depths will forward packets most of the time and their energy will soon run out, causing them to die. To address the energy loss by DBR, an energy-saving protocol was designed [30]. This protocol takes energy as one of the conditions of routing and forwarding to extend the running cycle of the network. All the methods discussed above can reduce network energy loss, but they ignore the distribution position of nodes in actual situations, resulting in network communication interruptions, unbalanced energy consumption in the process of data forwarding, and waste of node resources.

In summary, unlike the modeling environment on the ground, the underwater environment is an open dynamic area. There are many difficulties in constructing the UWSNs due to the undulating terrain of the seabed and the hydraulic effects of water flow. To solve the coverage control problem of nodes, the following problems need to be addressed: (1) The limited energy carried by underwater nodes and the mobility of underwater nodes cause deformation of the topology of UWSNs, leading to coverage holes in some areas, thus affecting the quality of service. (2) The existing covering research involves mainly the geometric method or the use of node force between particles. The former has poor operability in the underwater environment, while the latter is prone to some coverage fluctuations during final network operation. (3) To ensure that the UWSNs cover as few holes as possible, it is necessary to introduce artificial intelligence optimization algorithms to drive underwater nodes to appropriate positions.

Given that there are many covered holes in underwater networks in the dynamic open underwater environment, this study makes full use of the combination of particle swarm optimization (PSO) and VFA to propose a three-dimensional iterative enhanced underwater covered hole recovery method. For this article, we make the following contributions: (1) Put forward the improved PSO strategy for complete underwater node deployment, design the iterative steps for nonlinear decreases, and automatically adjust the inertia weight and acceleration factor. It can achieve a balance between local and global search capabilities. (2) To avoid the problem of local optima in the search algorithm, underwater nodes are considered as particles to calculate their mutual forces, driving them to move towards positions that can increase coverage rate. Disturbance operations are carried out in the later stages of iteration to weaken the oscillations of coverage rate. (3) Experimental studies on network topology, coverage rate, coverage efficiency, coverage holes, and average remaining energy before and after utilization of the proposed coverage algorithm were conducted. In terms of enhancing UWSN coverage, the proposed coverage algorithm was verified to be superior to BES, 3D-IVFA, and DABVF.

The remainder of this article is structured as follows. Section 2 presents a three-dimensional iterative enhancement coverage algorithm; Section 3 evaluates multiple experiments for various performance metrics; Section 4 gives the conclusions.

2. Proposed Coverage Enhancement Modeling

Using the advantages of particle swarm optimization and virtual force, we proposed a three-dimensional iterative enhancement for coverage hole recovery in UWSNs, as shown in Figure 1. First, the initial deployment of underwater nodes adopts an improved optimization search algorithm, and then virtual force is introduced to make underwater sensors move towards positions of greatest coverage. To avoid oscillations in the late iteration, the global interference mechanism is used to change the direction of particle motion.

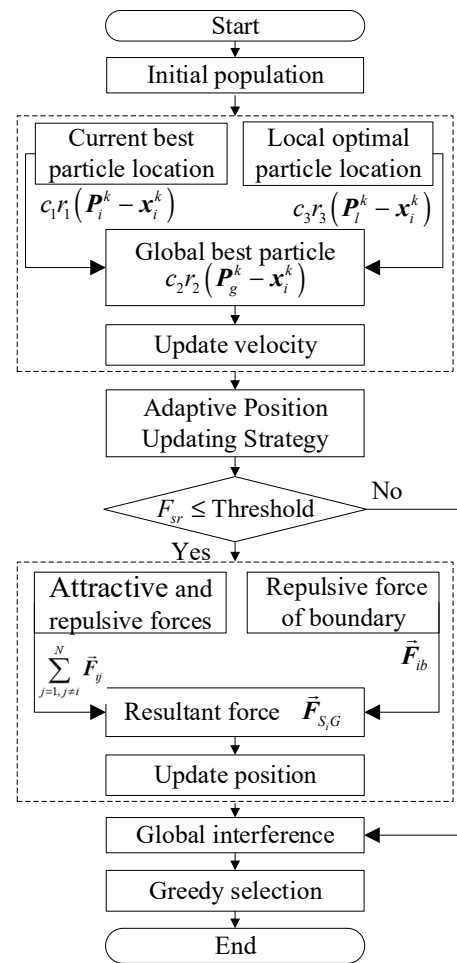


Figure 1. The overall architecture of the proposed coverage algorithm.

2.1. Coverage Description and Node Motion Model

To make the problem easier to solve, the monitoring area is defined as $L \times W \times H$, with several M cubic grids. The center point of each cubic grid corresponds to a grid dot, and all grid dots constitute the UWSNs. Defining G_w as the w^{th} grid point, the sets of all grid dots is represented by $G = \{G_1, G_2, \dots, G_w, \dots, G_M\}$, where $G_w = (x_w, y_w, z_w)$. There are N underwater nodes deployed in the UWSNs. Defining S_i as the i^{th} underwater node, the sets of all underwater nodes are expressed as $S = \{S_1, S_2, \dots, S_i, \dots, S_N\}$, where $S_i = (x_i, y_i, z_i)$. The sphere-sensing area of each underwater node has the same sensing radius whose sphere center is the node coordinates. The Euclidean distance $d(S_i, G_w)$ between the underwater node S_i and the grid dot G_w is expressed as

$$d(S_i, G_w) = \|S_i - G_w\| \tag{1}$$

where $\|\cdot\|$ is a binary norm indicating the distance between points. Based on the Boolean perception model, the probability $P_{G_w}(S_i)$ that the grid point G_w is perceived by the underwater node S_i is expressed as

$$P_{G_w}(S_i) = \begin{cases} 1 & d(S_i, G_w) \leq R_s \\ 0 & d(S_i, G_w) > R_s \end{cases} \tag{2}$$

where R_s is the sensing radius of the underwater node. If $P_{G_w}(S_i)$ is equal to 1, the grid point G_w is covered by the underwater node S_i ; otherwise, the grid point G_w is a coverage hole. Hence, the joint sensing probability $P_{G_w}(S)$ by all underwater nodes S is expressed as

$$P_{G_w}(S) = 1 - \prod_{i=1}^N (1 - P_{G_w}(S_i)) \tag{3}$$

In UWSNs, the underwater nodes are affected by environmental factors such as underwater currents, tides, and wind, and their positions change, to some extent [31]. Therefore, it is crucial to analyze the movement of underwater nodes. The oceans in Physical Oceanography and Pure Kinematics are viewed as homogeneous fluids of rotation that manifest themselves as layers in terms of density. Horizontal flows occur in nearly unperturbed fashion at every point due to vertical flows; thus, such motions display a finite damp behavior. When the node moves in UWSNs with node drift, the coverage of the node also changes. Therefore, it is necessary to introduce a water flow model that conforms to the actual situation. As deep-sea environments are often highly complex, the meandering current mobility model (MCM) [32] is used to establish the motion model for underwater nodes under ocean currents, tides, and other marine environmental conditions. All plane motions that cannot be compressed can be represented by the fluid equation $\varphi(x, y, t)$. This model was also used in this study to predict the velocity of point i and the coordinate positions (x_i, y_i, z_i) in the horizontal direction at time t . Nodes are initially distributed unevenly in the surveillance zone, and their positions change in the mobility model given in the following equation [33]:

$$\varphi(x, y, t) = -\tanh \left[\frac{y - B(t) \sin(k(x - ct))}{\sqrt{1 + k^2 B(t)^2 \cos^2(k(x - ct))}} \right] \tag{4}$$

$$B(t) = A + \varepsilon \cos(\omega t) \tag{5}$$

where A is the average meander width; k is the number of bends per unit length; c is the displacement rate of ocean current in direction Y ; $B(t)$ is the width of the control curve; ε is used to control the amplitude of the entire ocean current field; and ω is the frequency of the ocean current in the flow field. In general, attention is only paid to the movement of nodes in the X and Y directions, and the variability in the vertical direction is ignored. Therefore, the following analytical formulae are used to define the speeds of motion in the X and Y directions:

$$v_X = -\frac{\partial \varphi(x, y, t)}{\partial y} \tag{6}$$

$$v_Y = \frac{\partial \varphi(x, y, t)}{\partial x} \tag{7}$$

To simplify the formula, $a = y - B(t) \sin(k(x - ct))$ and $b = 1 + k^2 B(t)^2 \cos^2(k(x - ct))$. The two velocity components of the node motion to the east and north can be simplified to

$$v_X = \left[1 - \tanh\left(\frac{a}{b}\right) \right] \cdot (b)^{0.5} \tag{8}$$

$$v_Y = \left[1 - \tanh^2\left(\frac{a}{b}\right) \right] \cdot \left[\frac{B(t)k \cos(k(x - ct))}{b^{0.5}} - \frac{k^3 B^2(t) \sin(2k(x - ct)) \cdot a}{2 \cdot b^{1.5}} \right] \tag{9}$$

Based on the above node motion model, when the time passes Δt , the node moves $\sum_1^t v_X \cdot \Delta t$ m in the X direction and $\sum_1^t v_Y \cdot \Delta t$ m in the Y direction. The node is mainly affected by gravity and buoyancy in the Z direction. Initially, the gravity of the node is greater than its buoyancy, and the node is in a sinking state. However, considering that the final state of the node is located in water, that is, gravity equals buoyancy, the displacement

of the node in the Z direction does not change under the strong impact of the horizontal direction flow. After Δt , the position of underwater node i is

$$(x'_i, y'_i, z'_i) = \left(x_i + \sum_1^t v_X \cdot \Delta t, y_i + \sum_1^t v_Y \cdot \Delta t, z_i\right) \tag{10}$$

2.2. Enhanced Coverage and Protocol Modeling

The distribution of underwater nodes can get too dense or too sparse when affected by the random distribution of sensor nodes and water flow force, leading to poor coverage and more coverage holes in the sensor networks. Therefore, underwater nodes need to be deployed to improve coverage rate and reduce coverage holes in as many grid points as possible [34]. With the expansion of the application of artificial intelligence algorithms to UWSNs, the underwater nodes are considered as particles and the improved PSO is used for UWSN deployment. Each particle is guided to the optimal path and its particle best (*pbest*) and global best (*gbest*) positions are obtained in the solution set to discover a better position. To search for more accurate particle positions, the entire population is divided into several groups and the particle with the best fitness in several groups is called *lbest*. At the k^{th} iteration, the particle velocity is determined by the optimal position of the i^{th} particle search P_i^k , the locally best position within several groups P_l^k , and its overall best position P_g^k [35]. The formula for updating the velocity of a particle is

$$v_i^{k+1} = \omega^k v_i^k + c_1 r_1 (P_i^k - x_i^k) + c_2 r_2 (P_g^k - x_i^k) + c_3 r_3 (P_l^k - x_i^k) \tag{11}$$

where $r_1, r_2,$ and r_3 are random numbers in the interval $[0, 1]$; $c_1, c_2,$ and c_3 are acceleration coefficients; v_i^k and x_i^k are the particle velocity and position at the k^{th} iteration; v_i^{k+1} is the updated particle velocity and position at the $(k + 1)^{\text{th}}$ iteration; ω^k is the inertia weight factor that affects the particle inheritance proportion of current velocity. Particles with high speeds are beneficial for enhancing the global search ability, while particles with low speeds can improve the local search performance. To balance the local and global abilities, a nonlinearly decreasing adaptive inertia weight factor needs to be designed [36]. In the early iteration stage, it is possible to search large regions. In the later iteration stage, the local convergence needs to be enhanced to the global optimum. The inertia weight factor is expressed as

$$\omega^k = \omega_{\min} + \frac{\omega_{\max} - \omega_{\min}}{1 + e^{-(0.2 \times (K - k) - 10)}} \tag{12}$$

where ω_{\min} denotes the minimum inertia weight factor, usually set to 0.9; ω_{\max} denotes the maximum inertia weight factor, usually set to 0.4; K is the maximum iteration number; and k denotes the current iteration number. In addition to the inertia weight factor, the acceleration coefficients can cause particles to cluster within a certain phase or cause premature convergence to a local optimum. As a result, different particles are generated, resulting in particles with different search capabilities. To improve the convergence speed, c_1 and c_3 gradually decrease with iteration number while c_2 gradually increases with iteration number. This can be expressed as [37]

$$\begin{cases} c_1 = c_{1\min} - (c_{1\min} - c_{1\max}) \frac{k}{K} \\ c_2 = c_{2\min} + (c_{2\max} - c_{2\min}) \frac{k}{K} \\ c_3 = c_{3\min} - (c_{3\min} - c_{3\max}) \frac{k}{K} \end{cases} \tag{13}$$

where $c_{1\min}$ and $c_{1\max}$ denote the minimum and maximum values of acceleration coefficient c_1 ; $c_{2\min}$ and $c_{2\max}$ denote the minimum and maximum values of acceleration coefficient c_2 ; $c_{3\min}$ and $c_{3\max}$ denote the minimum and maximum values of acceleration coefficient c_3 . Different position update strategies can search for better solutions with higher efficiency, and an adaptive position update strategy is designed based on the ratio E_i of the particle current fitness to the population average fitness. When the ratio E_i is small, the particle performance is higher than the population average performance, while when the ratio

E_i is large, the population average performance is higher than the particle performance. Therefore, the adaptive position update strategy can be expressed as

$$x_i^{k+1} = \begin{cases} \omega^k x_i^k + (1 - \omega^k) v_i^{k+1} + rand \cdot P_g^k \cdot \omega^k & E_i > rand \\ x_i^k + v_i^{k+1} & \text{otherwise} \end{cases} \quad (14)$$

where the ratio E_i is written as $\frac{\exp(\text{fit}(x_i^{k+1}))}{\exp(\frac{\sum_{i=1}^n \text{fit}(x_i^{k+1})}{n})}$; $\text{fit}(\cdot)$ is the particle fitness function; and

n is the number of particle populations. However, underwater node coverage based on artificial intelligence search is prone to falling into local optimal. Virtual forces are used to mutate the optimal position and the underwater node position is updated by comparing the optimal values before and after the mutation. Underwater nodes are abstracted as particles in the potential field, and corresponding repulsive and attractive forces are generated by comparing the geometric distance of the nodes with the threshold. At the same time, there is a repulsive force between the underwater node and the boundary region. Under the combined action of three forces, underwater nodes distributed in dense or sparse areas are driven to move in the direction of a higher coverage rate. Based on Coulomb law, the virtual force \vec{F}_{ij} between the i^{th} and j^{th} nodes is expressed as

$$\vec{F}_{ij} = \begin{cases} (\epsilon_a(d_{ij} - d_{th}), \alpha_{ij}), & \text{if } d_{th} < d_{ij} \leq R_c \\ 0, & \text{if } d_{ij} > R_c \text{ or } d_{th} = d_{ij} \\ (\epsilon_r(\frac{1}{d_{th}^2} - \frac{1}{d_{ij}^2}), \alpha_{ij} + \pi), & \text{if } d_{ij} < d_{th} \end{cases} \quad (15)$$

where ϵ_r is the repulsive force coefficient; ϵ_a is the attractive force coefficient; d_{ij} is the geometric distance between nodes; d_{th} is the distance threshold; R_c is the communication radius of the underwater node; and α_{ij} is the azimuth angle between nodes. The distribution density of underwater nodes causes the distance between nodes to be too far or too close, resulting in corresponding repulsive or attractive forces between nodes. It is easy to reduce the node coverage efficiency when there are many underwater nodes clustered in the boundary area. The repulsive force \vec{F}_{ib} between underwater nodes and the boundary can be calculated as

$$\vec{F}_{ib} = \begin{cases} (\frac{\epsilon_b}{(d_{thb} - d_{ib})^2}, \alpha_{ib} + \pi), & \text{if } d_{ib} < d_{thb} \\ 0, & \text{otherwise} \end{cases} \quad (16)$$

where d_{thb} is the distance threshold between the underwater node and the boundary area; d_{ib} is the geometric distance between the underwater node and the boundary area; ϵ_b is the repulsive force coefficient; and α_{ib} denotes the azimuth angle. When the geometric distance between the underwater node S_i and the grid point G_w is larger than the sensing radius R_s and smaller than $\sqrt{3}R_s$, the attractive force is generated and expressed as

$$\vec{F}_{S_i G_w} = \begin{cases} \epsilon_d(\|S_i - G_w\| - R_s), & \text{if } R_s \leq \|S_i - G_w\| < \sqrt{3}R_s \\ 0, & \text{otherwise} \end{cases} \quad (17)$$

where $\|S_i - G_w\|$ is the Euclidean distance between the underwater node S_i and the grid dot G_w ; ϵ_d is the attractive force coefficient; and $\vec{F}_{S_i G_w}$ is the attractive force from underwater node S_i to the grid dot G_w . The combined force $\vec{F}_{S_i G}$ of all grid points on the underwater node S_i is expressed as

$$\vec{F}_{S_i G} = \sum_{w=1}^M \vec{F}_{S_i G_w} \quad (18)$$

In summary, the total virtual force \vec{F} on underwater node S_i is expressed as

$$\vec{F} = \sum_{j=1, j \neq i}^N \vec{F}_{ij} + \vec{F}_{ib} + \vec{F}_{S_i, G} \tag{19}$$

where j represents neighboring underwater nodes. Virtual forces act on randomly distributed underwater nodes, causing them to move towards sparse areas from dense areas, thereby maximizing the coverage rate. The underwater node moves from its initial position to the final position under the action of virtual forces, which can be expressed as

$$x_{new} = \begin{cases} x_{old}, & \text{if } \left| \vec{F}_x^i \right| \leq \vec{F}_{th} \\ x_{old} + \frac{\vec{F}_x^i}{\vec{F}_i} \times \eta \times e^{-\frac{1}{\vec{F}_i}}, & \text{if } \left| \vec{F}_x^i \right| > \vec{F}_{th} \end{cases} \tag{20}$$

$$y_{new} = \begin{cases} y_{old}, & \text{if } \left| \vec{F}_y^i \right| \leq \vec{F}_{th} \\ y_{old} + \frac{\vec{F}_y^i}{\vec{F}_i} \times \eta \times e^{-\frac{1}{\vec{F}_i}}, & \text{if } \left| \vec{F}_y^i \right| > \vec{F}_{th} \end{cases} \tag{21}$$

$$z_{new} = \begin{cases} z_{old}, & \text{if } \left| \vec{F}_z^i \right| \leq \vec{F}_{th} \\ z_{old} + \frac{\vec{F}_z^i}{\vec{F}_i} \times \eta \times e^{-\frac{1}{\vec{F}_i}}, & \text{if } \left| \vec{F}_z^i \right| > \vec{F}_{th} \end{cases} \tag{22}$$

where $x_i^{k+1} = (x_{old}, y_{old}, z_{old})$ are the optimal coordinates of underwater nodes generated by improved particle swarm optimization; $x'_i = (x_{new}, y_{new}, z_{new})$ are the final coordinates of underwater nodes after using virtual force; \vec{F}_x^i, \vec{F}_y^i , and \vec{F}_z^i are the virtual force components on the nodes i ; η is the moving step coefficient. The optimization tends to fall into the local optimal in the late iteration, thus global interference is introduced to change the particle motion mode [38]. The optimal particle position is defined as [39]

$$x''_i = rand \cdot x'_i + (1 - rand) \cdot (x'_i - (P_u^k)) \tag{23}$$

$$x'''_i = \begin{cases} x''_i & \text{fit}(x''_i) < \text{fit}(x'_i) \\ x'_i & \text{otherwise} \end{cases} \tag{24}$$

where P_u^k is any individual particle position, $u = rand([0, n])$; x''_i is the new particle position generated; and x'''_i is the particle position updated by the interference mechanism.

To find out more about how well the algorithm performs in terms of energy, based on the node location obtained by the coverage algorithm, the energy efficiency of UWSN nodes is analyzed using the clustering algorithm and the routing protocol with depth information as the forwarding condition. To better judge whether the node has the forwarding condition, the depth threshold parameter is introduced. When the sensor node receives a packet, the node first compares its depth difference with the previous hop node. If the candidate node is near the receiving node, that is, the depth difference is less than the threshold, the candidate node is considered qualified to forward packets; otherwise, the candidate node discards the packet directly. To prevent redundant packet transmission, the packet forwarding priority method is adopted. The packet forwarding priority depends on the estimated packet sending time ST ; the earlier the estimated packet sending time of a node, the higher the packet forwarding priority. The estimated packet sending time ST is associated with the packet retention time HT and the packet receiving time RT , that is,

$ST = RT + HT$. When a candidate relay node comes across the information package, it delays forwarding it until it compares its holding period HT , that is, the forwarding delay of the packet. Packets are scheduled for forward forwarding based on their retained times at each node. Shorter holding times result in greater forwarding priority for nodes, thus packets are forwarded first. The HT calculation is associated with the depth difference, Δd , between nodes [29]:

$$HT = \frac{2\tau}{\delta}(R - \Delta d) \tag{25}$$

where Δd is the depth difference between the candidate node and the previous hop node; R is the maximum communication range of the node; $\tau = \frac{R}{v}$, v represents the acoustic velocity in water; and δ is the global constant. When δ is small, node HT is longer, fewer nodes participate in packet forwarding, and less energy is consumed.

In the traditional DBR routing protocol, all nodes keep working and are ready to receive data packets at any time; this wastes a lot of node energy. This study proposes a DBR routing protocol based on location clustering. Considering the distribution of node positions, the monitoring area is divided into four equal small areas based on clustering. First, in each local small area, the routing protocol is used to transmit data packets to a relay node, and the remaining energy of each node is calculated at the end of the network operation. The data packets received by the relay nodes in each local small area are then sent to the sink node. Finally, the average remaining energy of the nodes is calculated. The average residual energy of nodes can be calculated as

$$E_{average} = \frac{\sum(E_{initial} - E_{consume})}{N} \tag{26}$$

where $E_{average}$ is the average remaining energy; $E_{initial}$ is the initial energy; $E_{consume}$ is the energy lost by the node; and N is the number of nodes.

3. Numerical Evaluations and Experimental Analyses

3.1. Parameter Settings

This study used the MATLAB R2021b software platform to implement the proposed algorithm, which was validated using simulated experimental validation. The length L , width W , and height H of the monitoring area are 500 m; the sensing radius R_s of the node is 100 m; the radius R_c of node communication is 200 m; the maximum number K of iterations is 100; the number n of particles swarm is 50; the number N of nodes is 25–50; the maximum inertia weight w_{max} is 0.9, the minimum inertia weight w_{min} is 0.4; acceleration factors $c_{1min} = 0.25$, $c_{1max} = 2.75$, $c_{2min} = 1.25$, $c_{2max} = 2.5$, $c_{3min} = 0.25$, and $c_{3max} = 2.75$; the maximum step length of sensor node movement under the action of grid point is $max_step = 2.5/2$; the maximum step length of sensor node movement under the action of sensor node is $max_sensor = 3.5/2$; node initial energy is 100 J; and the transmitting power, receiving power, and idle power of the node are 2 w, 0.75 w, and 0.001 w, respectively. To verify the effectiveness of the algorithm, the proposed algorithm was compared with the BES [20], 3D-IVFA [22], and DABVF [24] algorithms under the same parameter conditions. The simulation performance of the proposed algorithm was compared with those of BES-DBR, 3D-IVFA-DBR, and DABVF-DBR on the NS-3 software platform. The results verified that network energy loss can be effectively reduced.

3.2. Simulation Results and Analysis

Figure 2 shows the coverage effect of 45 nodes randomly distributed within the monitoring range. The number of nodes randomly placed in each part of the network is not equal, resulting in poor network coverage, with a coverage rate of only 72.02%. Figure 3 shows the network coverage optimization effect of node redeployment by the proposed algorithm. The nodes of a more balanced density distribution are obvious. The optimized network coverage rate reached 91.36%, with the coverage rate increasing by 19.34%. The main reason lies in node pre-coverage using the improved particle swarm

optimization algorithm and then using virtual force to drive nodes to move toward the coverage blind spot, improving the balanced distribution of underwater wireless sensor nodes and effectively reducing the coverage hole.

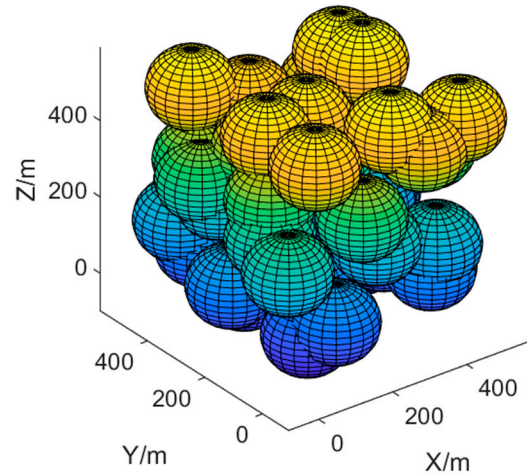


Figure 2. Initial network layout.

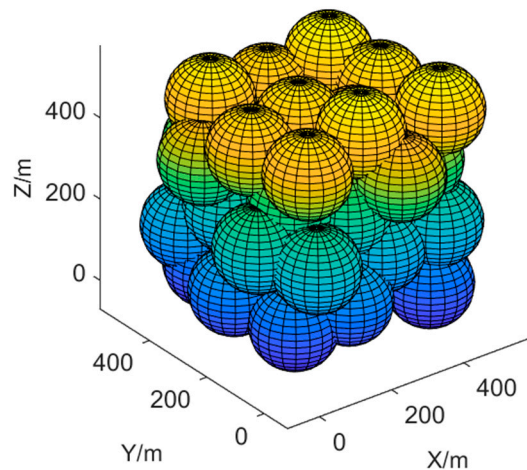


Figure 3. Final network layout.

Figure 4 shows the comparisons of changes in coverage ratios of different coverage algorithms as the node number changes. When the node number increases from 25 to 50 in increments of 5, the network coverage increases successively. The network coverage of random node distributions increased from 43.80% to 53.05%, 57.12%, 57.96%, 72.02%, and 72.10%. We can see from the figure that the underwater node number is directly associated with network coverage. The network coverage value increases as the node number increases, improving the coverage effect of the network and meeting its coverage requirements. However, the cost of network coverage will also increase. With 45 underwater sensor nodes deployed as the research object, the coverage rates for BES, 3D-IVFA, DABVF, and the proposed algorithm are 83.28%, 88.85%, 89.31%, and 91.36%, respectively, after 100 iterations. The proposed algorithm is better than BES, 3D-IVFA, and DABVF in coverage by about 8.06%, 2.51%, and 2.05%, respectively. The above quantitative analysis shows that the proposed algorithm can greatly increase the coverage rate, which is also the embodiment of the superiority of the algorithm. The reason is that the algorithm combines the improved PSO and VFA algorithms to make use of their complementary advantages so that the layout of nodes can be adjusted quickly to obtain the best results and achieve the best coverage of the network.

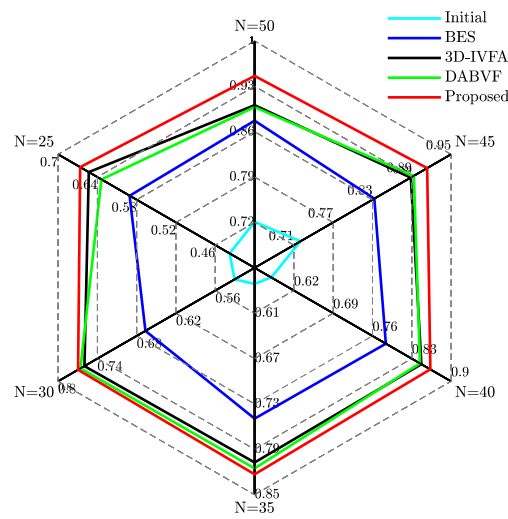


Figure 4. Comparison of coverage rate optimization of different coverage algorithms with changes in node numbers.

In Figure 5, we can see that as the node number changes, both the initial coverage and the final coverage of the algorithm in this study show the same upward or downward trends. More nodes can achieve greater coverage, but if the nodes are randomly distributed, the expected coverage results cannot be achieved. The reason for the improved coverage after optimization of the proposed algorithm is that the improved PSO is used for node pre-coverage and virtual force is then introduced to mutate the optimal coverage position. In the subsequent iteration, the global interference mechanism is introduced to get a more suitable node position. These strategies overcome the defect that the previous algorithm easily falls into the optimal solution, accelerates the search speed of the target value, and achieves higher coverage.

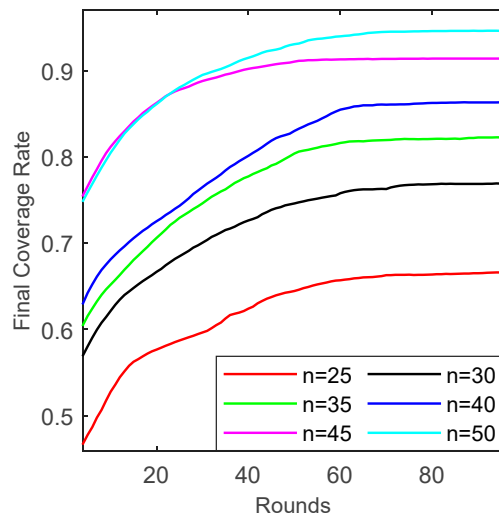


Figure 5. The relationship between coverage rate and node number in the proposed algorithm.

In Figure 6, we can see that the node number and coverage efficiency show opposite upward or downward trends. The reason is that the more the number of nodes, the greater the probability of overlap between nodes, resulting in network coverage redundancy increases, which reduces the utilization rate of the node. With 45 underwater sensor nodes deployed as the research object, the node coverage efficiency of the proposed algorithm is significantly better than those of BES, 3D-IVFA, and DABVF algorithms, which are

improved by 1.36%, 1.67%, and 5.36%, respectively. From the above quantitative analysis, the proposed algorithm performs better, especially in making full use of the nodes.

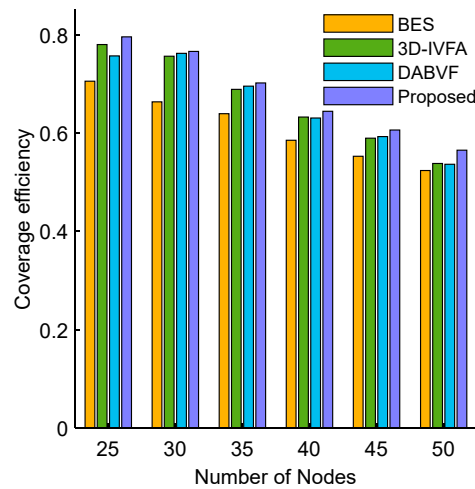


Figure 6. The relationship between coverage efficiency and node number in the four algorithms.

In Figure 7, With 45 underwater sensor nodes deployed as the research object, figure (a1–a3), (b1–b3), (c1–c3) and (d1–d3) shows the moving trajectories, final node positions, and final node coverage effects of the four algorithms: BES, 3D-IVFA, DABVF, and proposed algorithm. In the figure, dots represent the random distribution positions of nodes, pentagons represent the positions of nodes after optimization, the line between the point and the five-pointed star represents the movement trajectory of nodes from the random distribution position to the optimized position, and the area shaped by the ball represents the perception range of underwater nodes. We can see that the proposed algorithms show excellent performance of nodes distributed uniformly compared with the other three methods. This is because the proposed algorithm uses an adaptive position update mechanism that can autonomously choose the most suitable strategy to update the particle positions. The global exploration ability of the algorithm is enhanced while at the same time, the local development ability of the algorithm is ensured. In addition, the VFA algorithm is used to drive nodes to the optimal position using the force between nodes, which reduces the coverage blind area of the network and optimizes the coverage effect of the network.

In Figure 8, 3D-IVFA has the best average iteration step performance. Because 3D-IVFA extends the traditional law of virtual force, the use of the center of gravity and balance force makes the deployment of sensor nodes more reasonable, reducing the movement of large distances between nodes. The proposed algorithm has worse performance in the average iteration step than the BES, 3D-IVFA, and DABVF algorithms. This is because the algorithm constantly updates the node position in the running process and adopts the greedy strategy to select the node position again through the global interference mechanism in the late iteration, resulting in large moving distances between nodes. This is because of the constant update of node positions constantly seeking the optimal position, improving the balance of distribution density, and achieving the best coverage effect.

In Figure 9, moving displacements of 45 underwater sensor nodes are projected from three mutually perpendicular directions. The dots represent the random distribution positions, the pentagrams represent the optimized positions, and the lines between the points and the pentagrams represent the 3D views of the moving displacements from the random distribution position to the optimized position. Figure (a1), (b1), (c1), and (d1) shows the front views of the node motion trajectories of BES, 3D-IVFA, DABVF, and the proposed algorithm, respectively. Figure (a2), (b2), (c2), and (d2) shows the right elevations of the node motion trajectories of BES, 3D-IVFA, DABVF, and the proposed algorithm, respectively. Figure (a3), (b3), (c3), and (d3) shows the top views of the node motion trajectories of BES, 3D-IVFA, DABVF, and the proposed algorithm, respectively. We can see that, compared

with the other three algorithms, the proposed algorithm is better when an equal distribution of nodes is considered from a three-dimensional perspective. This is because the proposed algorithm uses strategies such as improved PSO and global interference mechanism to constantly update the location of nodes to make their distribution more uniform and realize optimal deployment of the network.

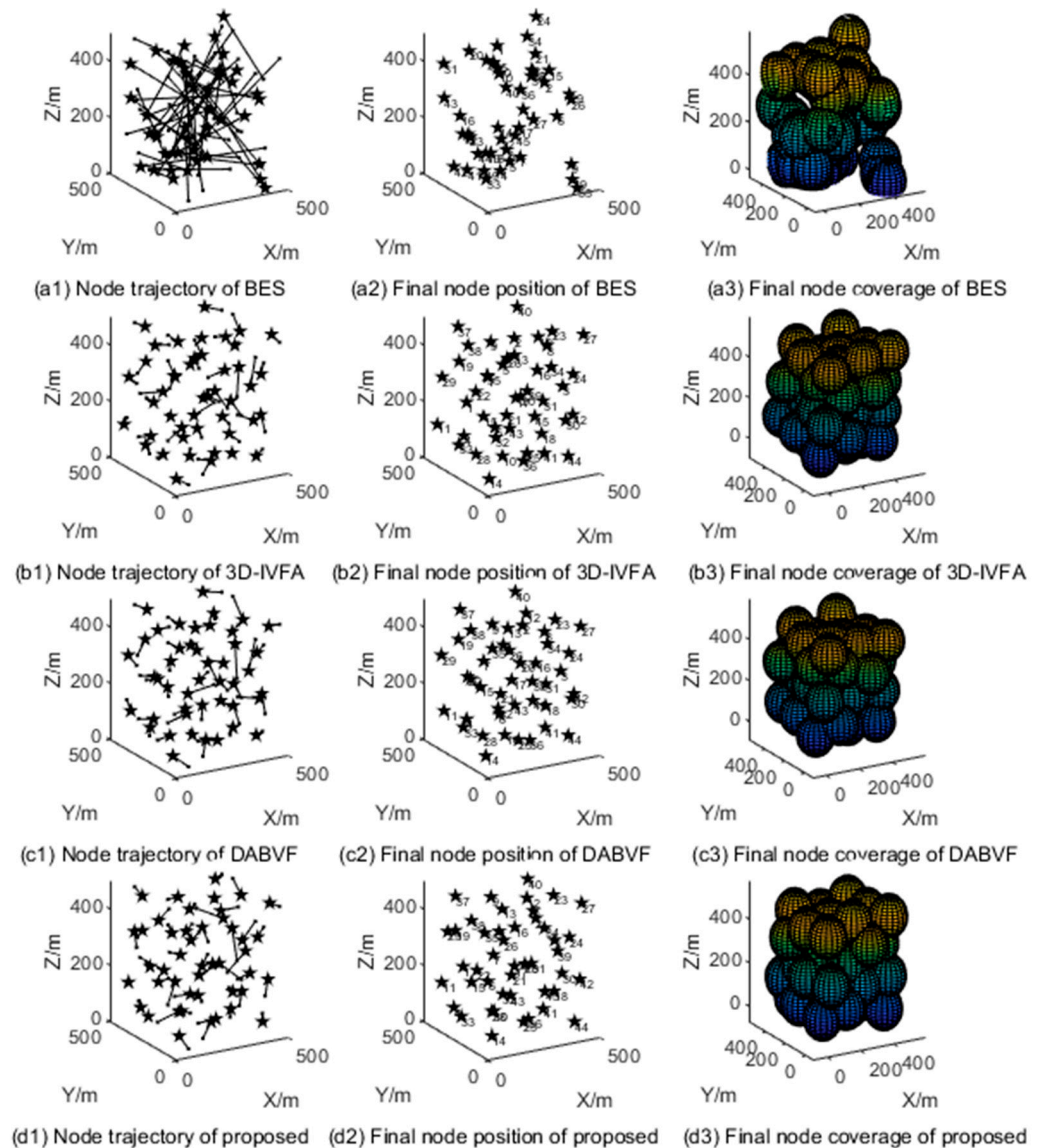


Figure 7. Node motion trajectory and final coverage diagram.

Figure 10 shows the comparison of k -coverage before and after the optimization of the proposed algorithm using different node numbers. After optimization of the proposed algorithm, the coverage of multiple repetitions decreases while the coverage of low repetitions increases. For example, with 45 underwater sensor nodes deployed as the research object, the 1-coverage and 2-coverage during the initial deployment are only 43.09% and 22.14%, respectively, and the coverage hole is 27%. After 100 iterations, 1-coverage and 2-coverage reaches 63.03% and 26.34%, respectively, while the covered hole is reduced to 8.62%. When node numbers increase from 25 to 50 in increments of 5, the coverage hole is 55.26%, 46.19%, 41.81%, 40.83%, 27%, and 27.19%, respectively. After 100 iterations, the coverage hole decreased from 33.38% to 23.05%, 17.72%, 13.69%, 8.62%, and 5.40%. Data analysis shows that the proposed algorithm can expand the effective coverage area and improve the overall performance and service level of the network. This is because the

algorithm is based on the virtual force applied to the node, which promotes the underwater node to move to the uncovered area, reduces the probability of overlapping node coverage, makes it reach the optimal position effectively, and improves the node utilization rate.

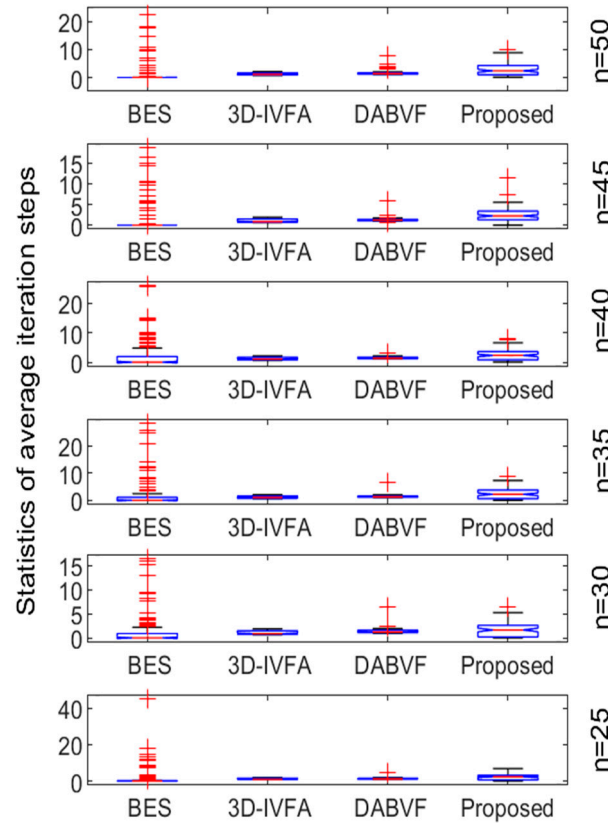


Figure 8. Comparison of average iteration steps of different algorithms.

In addition to validating the proposed algorithm using different node numbers, coverage efficiencies, node motion trajectories, coverage holes, and other aspects, the complexity of the algorithm is also an important performance index for evaluating the quality of the coverage algorithm. The computational complexity of BES, 3D-IVFA, DABVF, and the proposed algorithm in this study is $O(KN)$, $O(KN^2)$, $O(KN^2)$, and $O(KN^2)$, respectively, where K represents the number of iterations the algorithm runs, and N represents the number of sensor nodes. Compared with 3D-IVFA and DABVF, the proposed algorithm improves the coverage of the network without increasing the complexity of the algorithm.

Figure 11 shows changes in the average residual energy of nodes of the proposed algorithm and the other three algorithms as network time changes. We can see that the network running time and the average residual energy of nodes increase and decrease in the same direction. With 45 underwater nodes as the research object, the average residual energy of BES-DBR, 3D-IVFA-DBR, DABVF-DBR, and the proposed coverage algorithm are 57.67 J, 48.59 J, 45.30 J, and 72.74 J, respectively, when the simulation time is 200 s. The proposed algorithm is significantly better than BES-DBR, 3D-IVFA-DBR, and DABVF-DBR in terms of the average residual energy performance of nodes during network operation. At the same time, it also extends the network life cycle. This is because the algorithm adopts the DBR routing protocol, which is based on location clustering. Based on the location of nodes obtained using the coverage algorithm, the monitoring area is divided into four equal areas using clustering. To reduce information transmission energy loss between nodes, the method is first used to optimize the residual energy of nodes in each local small area. The average residual energy of nodes is then taken as the standard for comprehensive calculation.

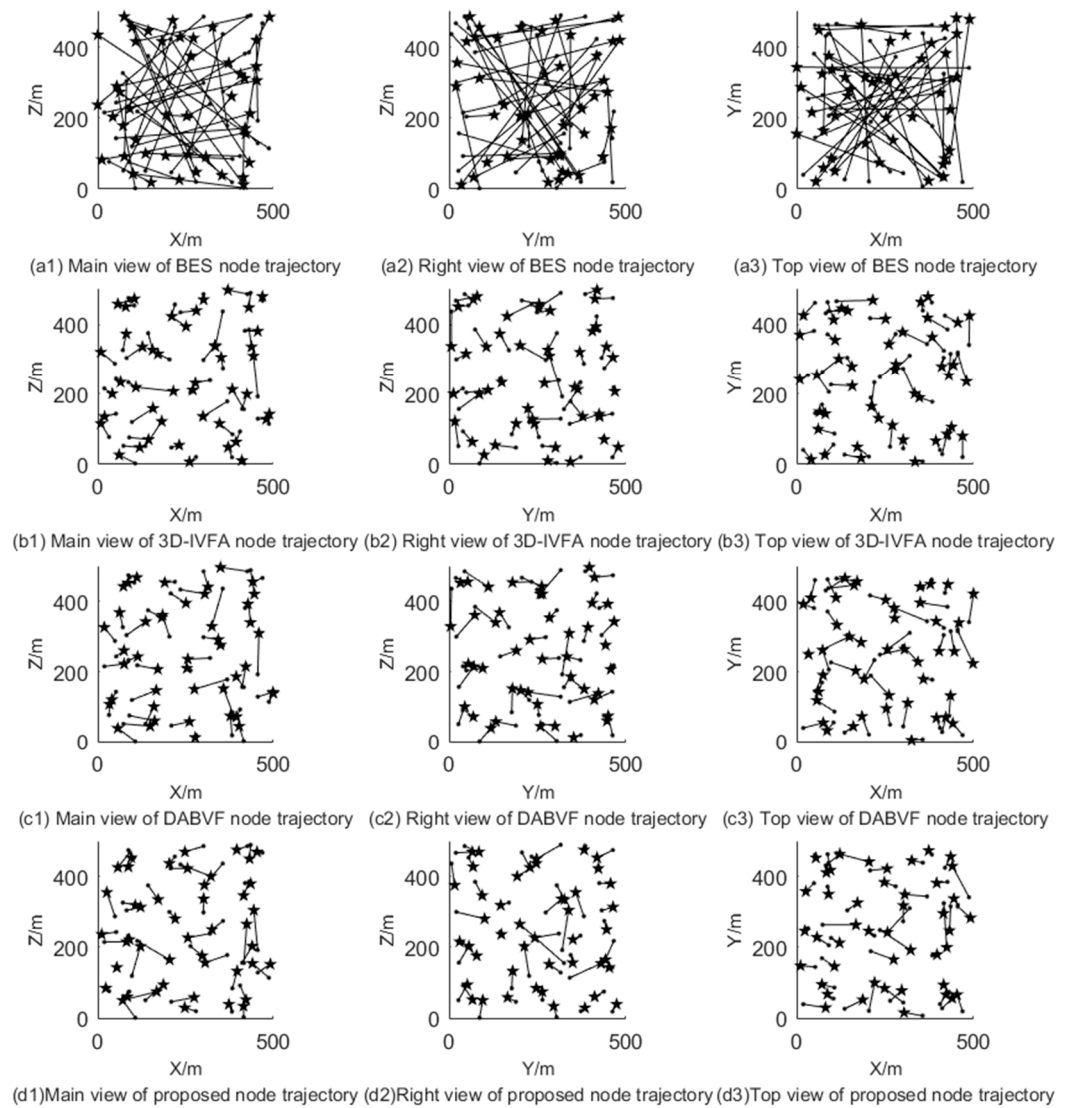


Figure 9. Three-dimensional view of four algorithms for node movement.

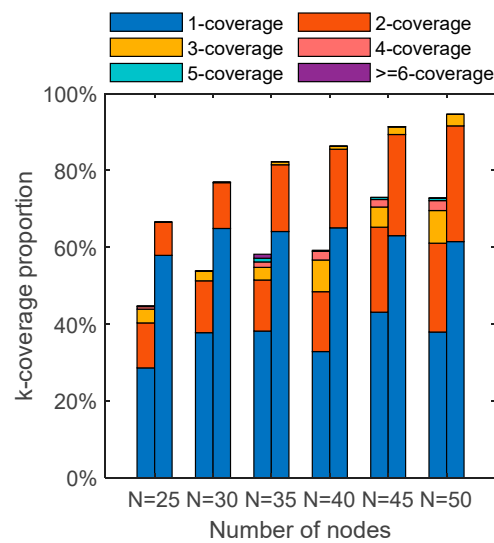


Figure 10. Comparison of k -coverage before and after optimization of the proposed algorithm.

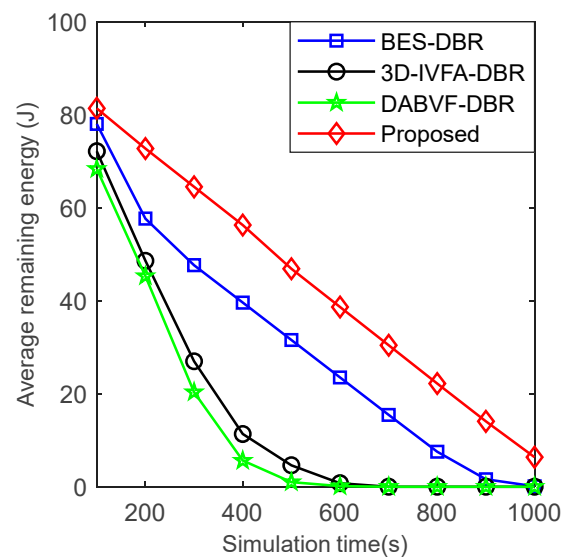


Figure 11. Relationship between the average residual energy of nodes and network simulation time.

4. Conclusions

Due to limited node resources, intelligent oceans require the highest possible coverage rate to ensure reliable networks in UWSNs. This study proposed a three-dimensional coverage hole recovery algorithm using improved PSO and VFA in UWSNs. To avoid the problem of search optimization algorithms falling into local optima and slow improvement of coverage in the later stages of iteration, pre-coverage of underwater nodes is first performed under improved particle swarm optimization; the nodes are then moved to a position with higher coverage under the action of virtual forces, including global mutation operations. The analysis of experimental data generated from 45 nodes showed that the coverage rate increased from 72.02% to 91.36% after using the proposed algorithm, effectively reducing the coverage hole. With 50 nodes deployed, the coverage rates for BES, 3D-IVFA, DABVF, and the proposed coverage algorithm increased to 87.69%, 90.08%, 89.80%, and 94.60%, while their corresponding coverage efficiencies were 53.62%, 53.79%, 52.36%, and 56.49%. In addition, we also verified that the clustering routing method based on the optimal location of nodes obtained using the coverage algorithm had the effect of prolonging the network life cycle. Based on a series of experiments, the proposed algorithm was shown to be superior to the relevant algorithms in terms of coverage and coverage efficiency and effectively improved the performance of UWSNs. In future research work, we plan to study sensor nodes with different sensing radii and networks with barriers to further optimize and improve the deployment strategy for underwater wireless sensor networks to meet more underwater sensor network design goals such as network lifetime and network connectivity.

Author Contributions: Conceptualization, L.Z. and C.L.; methodology L.Z. and C.L.; software, L.Z.; validation, L.Z.; formal analysis, L.Z. and C.L.; investigation, L.Z.; resources, L.Z.; data curation, L.Z.; writing—original draft preparation, L.Z.; writing—review and editing, C.L.; visualization, X.G., Y.C., and H.Z.; supervision, C.L.; project administration, C.L.; funding acquisition, G.X. and C.L. All authors have read and agreed to the published version of the manuscript.

Funding: This research was funded by the National Natural Science Foundation of China (62001195), the Basic Science (Natural Science) Research Project of Jiangsu Higher Education Institutions (18KJB460003, 21KJB460030), and the Applied Basic Research Programs of Changzhou (CJ20220026). The authors would like to thank the anonymous reviewers for their helpful comments, which have improved the quality of the paper.

Data Availability Statement: The data presented in this paper are available upon contacting the corresponding author.

Conflicts of Interest: The authors declare no conflict of interest.

References

- Jiang, J.; Han, G.; Lin, C. A survey on opportunistic routing protocols in the Internet of Underwater Things. *Comput. Netw.* **2023**, *225*, 109658. [\[CrossRef\]](#)
- Razzaq, A.; Mohsan, S.A.H.; Li, Y.; Alsharif, M.H. Architectural Framework for Underwater IoT: Forecasting System for Analyzing Oceanographic Data and Observing the Environment. *J. Mar. Sci. Eng.* **2023**, *11*, 368. [\[CrossRef\]](#)
- Truong, V.T.; Ha, D.B.; So-In, C. On the System Performance of Mobile Edge Computing in an Uplink NOMA WSN with a Multiantenna Access Point over Nakagami-*m* Fading. *IEEE/CAA J. Autom. Sin.* **2022**, *9*, 668–685. [\[CrossRef\]](#)
- Zhang, S.; Chen, H.; Xie, L. ASVMR: Adaptive Support-Vector-Machine-Based Routing Protocol in the Underwater Acoustic Sensor Network for Smart Ocean. *J. Mar. Sci. Eng.* **2023**, *11*, 1736. [\[CrossRef\]](#)
- Hajjej, F.; Hamdi, M.; Ejbali, R.; Zaied, M. A distributed coverage hole recovery approach based on reinforcement learning for Wireless Sensor Networks. *Ad Hoc Netw.* **2020**, *101*, 102082. [\[CrossRef\]](#)
- Yao, Y.D.; Wen, Q.; Cui, Y.P.; Zhao, F.; Zhao, B.Z.; Zeng, Y.P. Coverage Enhancement Strategy in WMSNs Based on a Novel Swarm Intelligence Algorithm: Army Ant Search Optimizer. *IEEE Sens. J.* **2022**, *22*, 21299–21311. [\[CrossRef\]](#)
- Pundir, S.; Wazid, M.; Singh, D.P.; Das, A.K.; Rodrigues, J.J.; Park, Y. Intrusion detection protocols in wireless sensor networks integrated to Internet of Things deployment: Survey and future challenges. *IEEE Access* **2019**, *8*, 3343–3363. [\[CrossRef\]](#)
- Wen, Q.; Zhao, X.Q.; Cui, Y.P.; Zeng, Y.P.; Chang, H.; Fu, Y.J. Coverage enhancement algorithm for WSNs based on vampire bat and improved virtual force. *IEEE Sens. J.* **2022**, *22*, 8245–8256. [\[CrossRef\]](#)
- Habibiyan, R.; Sabbagh, A.G. Connectivity analysis of 2D underwater optical wireless sensor networks using a geometric approach. *Ad Hoc Netw.* **2022**, *134*, 102910. [\[CrossRef\]](#)
- So-In, C.; Nguyen, T.G.; Nguyen, N.G. An efficient coverage hole-healing algorithm for area-coverage improvements in mobile sensor networks. *Peer—Peer Netw. Appl.* **2019**, *12*, 541–552. [\[CrossRef\]](#)
- Zhang, Z.; Tian, S.; Yang, Y. Node Depth Adjustment Based Target Tracking in Sparse Underwater Sensor Networks. *J. Mar. Sci. Eng.* **2023**, *11*, 372. [\[CrossRef\]](#)
- Wang, Z.; Wang, B. A novel node sinking algorithm for 3D coverage and connectivity in underwater sensor networks. *Ad Hoc Netw.* **2017**, *56*, 43–55. [\[CrossRef\]](#)
- Zhang, J.; Han, G.; Sha, J.; Qian, Y.; Liu, J. AUV-assisted subsea exploration method in 6G enabled deep ocean based on a cooperative pac-men mechanism. *IEEE Trans. Intell. Transp. Syst.* **2021**, *23*, 1649–1660. [\[CrossRef\]](#)
- Wei, L.; Song, X.; Zheng, X.; Wu, X.; Gui, G. Boundary node identification in three dimensional wireless sensor networks for surface coverage. *IEICE Trans. Inf. Syst.* **2019**, *102*, 1126–1135. [\[CrossRef\]](#)
- Yao, Y.; Hu, S.; Li, Y.; Wen, Q. A node deployment optimization algorithm of WSNs based on improved moth flame search. *IEEE Sens. J.* **2022**, *22*, 10018–10030. [\[CrossRef\]](#)
- Zhao, X.Q.; Cui, Y.P.; Gao, C.Y.; Guo, Z.; Gao, Q. Energy-efficient coverage enhancement strategy for 3-D wireless sensor networks based on a vampire bat optimizer. *IEEE Internet Things J.* **2019**, *7*, 325–338. [\[CrossRef\]](#)
- Yi, J.; Qiao, G.; Yuan, F.; Tian, Y.; Wang, X. Sensor Deployment Strategies for Target Coverage Problems in Underwater Acoustic Sensor Networks. *IEEE Commun. Lett.* **2023**, *27*, 836–840. [\[CrossRef\]](#)
- Zhang, Y.; Wang, M.; Liang, J.; Zhang, H.; Chen, W.; Jiang, S. Coverage enhancing of 3D underwater sensor networks based on improved fruit fly optimization algorithm. *Soft Comput.* **2017**, *21*, 6019–6029. [\[CrossRef\]](#)
- Fattah, S.; Ahmedy, I.; Idris, M.Y.I.; Gani, A. Hybrid multi-objective node deployment for energy-coverage problem in mobile underwater wireless sensor networks. *Int. J. Distrib. Sens. Netw.* **2022**, *18*, 15501329221123533. [\[CrossRef\]](#)
- Kapileswar, N.; Phani Kumar, P. Energy efficient routing in IOT based UWSN using bald eagle search algorithm. *Trans. Emerg. Telecommun. Technol.* **2022**, *33*, e4399. [\[CrossRef\]](#)
- Jiang, P.; Wang, X.; Liu, J. A sensor redeployment algorithm based on virtual forces for underwater sensor networks. *Chin. J. Electron.* **2018**, *27*, 413–421. [\[CrossRef\]](#)
- Li, X.; Ci, L.; Yang, M.; Tian, C.; Li, X. Deploying three-dimensional mobile sensor networks based on virtual forces algorithm. In Proceedings of the Advances in Wireless Sensor Networks: 6th China Conference, CWSN 2012, Huangshan, China, 25–27 October 2012; Revised Selected Papers 6; 2013; pp. 204–216.
- Wang, W.; Huang, H.; He, F.; Xiao, F.; Jiang, X.; Sha, C. An enhanced virtual force algorithm for diverse k-coverage deployment of 3D underwater wireless sensor networks. *Sensors* **2019**, *19*, 3496. [\[CrossRef\]](#)
- Liu, C.; Zhao, Z.; Qu, W.; Qiu, T.; Sangaiah, A.K. A distributed node deployment algorithm for underwater wireless sensor networks based on virtual forces. *J. Syst. Archit.* **2019**, *97*, 9–19. [\[CrossRef\]](#)
- Jun, W.; Haoyang, G. Virtual force field coverage algorithms for wireless sensor networks in water environments. *Int. J. Sens. Netw.* **2020**, *32*, 174–181. [\[CrossRef\]](#)
- Hu, Y.; Sun, Y.; Chen, L. The VF-PSO optimization algorithm for coverage and deployment of underwater wireless sensor network. *Indian J. Geo-Mar. Sci. (IJMS)* **2022**, *51*, 219–228.

27. Xie, P.; Cui, J.H.; Lao, L. VBF: Vector-based forwarding protocol for underwater sensor networks. In Proceedings of the NETWORKING 2006. Networking Technologies, Services, and Protocols; Performance of Computer and Communication Networks; Mobile and Wireless Communications Systems: 5th International IFIP-TC6 Networking Conference, Coimbra, Portugal, 15–19 May 2006; pp. 1216–1221.
28. Nicolaou, N.; See, A.; Xie, P.; Cui, J.H.; Maggiorini, D. Improving the robustness of location-based routing for underwater sensor networks. In Proceedings of the Oceans 2007-Europe, Aberdeen, Scotland, 18–21 June 2007; pp. 1–6.
29. Yan, H.; Shi, Z.J.; Cui, J.H. DBR: Depth-based routing for underwater sensor networks. In Proceedings of the NETWORKING 2008 Ad Hoc and Sensor Networks, Wireless Networks, Next Generation Internet: 7th International IFIP-TC6 Networking Conference, Singapore, 5–9 May 2008; pp. 72–86.
30. Wahid, A.; Kim, D. An energy efficient localization-free routing protocol for underwater wireless sensor networks. *Int. J. Distrib. Sens. Netw.* **2012**, *8*, 307246. [[CrossRef](#)]
31. Luo, C.; Wang, B.; Cao, Y.; Xin, G.; He, C.; Ma, L. A hybrid coverage control for enhancing UWSN localizability using IBSO-VFA. *Ad Hoc Netw.* **2021**, *123*, 102694. [[CrossRef](#)]
32. Tsai, P.H.; Tsai, R.G.; Wang, S.S. Hybrid localization approach for underwater sensor networks. *J. Sens.* **2017**, *2017*, 5768651. [[CrossRef](#)]
33. Caruso, A.; Paparella, F.; Vieira, L.F.M.; Erol, M.; Gerla, M. The meandering current mobility model and its impact on underwater mobile sensor networks. In Proceedings of the IEEE INFOCOM 2008—The 27th Conference on Computer Communications, Phoenix, Arizona, 13–18 April 2008; pp. 221–225.
34. Luo, C.; Cao, Y.; Xin, G.; Wang, B.; Lu, E.; Wang, H. Three-dimensional coverage optimization of underwater nodes under multiconstraints combined with water flow. *IEEE Internet Things J.* **2021**, *9*, 2375–2389. [[CrossRef](#)]
35. Singh, P.; Khosla, A.; Kumar, A.; Khosla, M. Optimized localization of target nodes using single mobile anchor node in wireless sensor network. *AEU-Int. J. Electron. Commun.* **2018**, *91*, 55–65. [[CrossRef](#)]
36. Liu, H.; Zhang, X.W.; Tu, L.P. A modified particle swarm optimization using adaptive strategy. *Expert Syst. Appl.* **2020**, *152*, 113353. [[CrossRef](#)]
37. Qi, X.; Li, Z.; Chen, C.; Liu, L. A wireless sensor node deployment scheme based on embedded virtual force resampling particle swarm optimization algorithm. *Appl. Intell.* **2022**, *52*, 7420–7441. [[CrossRef](#)]
38. Luo, C.; Yang, X.; Wang, L.; Xin, G.; Ge, X.; Kong, F.; Wang, B. A node deployment-aided intelligent optimization estimation for WSNs positioning refinement. *IEEE Trans. Instrum. Meas.* **2023**. [[CrossRef](#)]
39. Zhang, X.; Liu, H.; Zhang, T.; Wang, Q.; Wang, Y.; Tu, L. Terminal crossover and steering-based particle swarm optimization algorithm with disturbance. *Appl. Soft Comput.* **2019**, *85*, 105841. [[CrossRef](#)]

Disclaimer/Publisher’s Note: The statements, opinions and data contained in all publications are solely those of the individual author(s) and contributor(s) and not of MDPI and/or the editor(s). MDPI and/or the editor(s) disclaim responsibility for any injury to people or property resulting from any ideas, methods, instructions or products referred to in the content.